THE JOURNAL OF PHYSICAL CHEMISTRY A
A JOURNAL OF THE AMERICAN CHEMICAL SOCIETY

pubs.acs.org/JPCA

Article

Dependence of Intramolecular Hydrogen Bond on Conformational Flexibility in Linear Aminoalcohols

Published as part of the The Journal of Physical Chemistry A virtual special issue "Women Scientists in China".

Yuhui Li, Xinlang Yang, Yuanqin Yu,* Xiaoguo Zhou, Rui Zhang, Jin Sun, and Shilin Liu*

Cite This: *J. Phys. Chem. A* 2023, 127, 9013−9021

Read Online

ACCESS | Metrics & More | Article Recommendations | Supporting Information

ABSTRACT: Intramolecular hydrogen bonds (H-bonds) are abundant in physicochemical and biological processes. The strength of such interaction is governed by a subtle balance between conformational flexibility and steric effect that are often hard to predict. Herein, using linear aminoalcohols $NH_2(CH_2)_nOH$ (n = 2−5) as a model system, we demonstrated the dependence of intramolecular H-bond on the backbone chain length. With sensitive photoacoustic Raman spectroscopy (PARS), the gas-phase Raman spectra of aminoalcohols were measured in both N−H and O−H stretching regions at 298 and 338 K and explained with the aid of quantum chemistry calculations. For n = 2−4, two conformers corresponding to the O−H···N intramolecular H-bond and free OH were identified, whereas for n = 5, only the free-OH conformer was identified. Compared to free OH, a striking spectral dependence was observed for the intramolecular H-bonded conformer. According to the red shift of the OH-bonded band, the strongest intramolecular H-bond yields in n = 4, but the favorable chain length to form an intramolecular hydrogen bond at room temperature was observed in n = 3, which corresponds to a six-membered-ring in 3-aminopropanol. This is in good agreement with statistical analysis from the Cambridge Structural Database (CSD) that the intramolecular hydrogen bond is preferred when the six-membered ring is formed. Furthermore, combined with the calculated thermodynamic data at the MP2/aug-cc-pVTZ//M062X/6-311++G(d,p) level, the origin of decrease in intramolecular hydrogen-bond formation was ascribed to an unfavorable negative entropy contribution when the backbone chain is further getting longer, which results in the calculated Gibbs free energy optimum changing with increasing temperature from n = 4 (0−200 K) to n = 3 (200−400 K) and to n = 2 (above 400 K). These results will provide new insight into the nature of intramolecular hydrogen bonds at the molecular level and the application of intramolecular hydrogen bonds in rational drug design and supramolecular assembly.

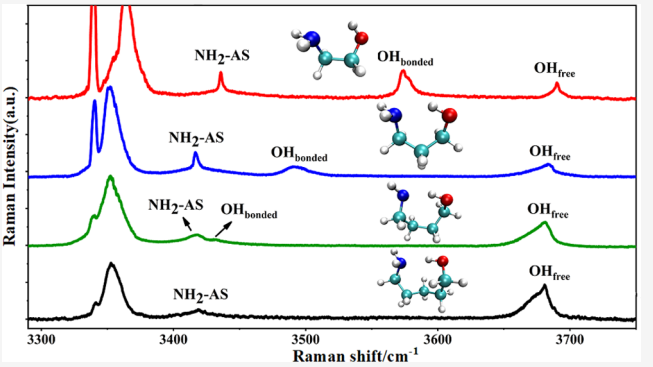

INTRODUCTION

Hydrogen bond (H-bond) is one of the most important driving forces in nature, playing a vital role in various physical, chemical, and biological processes, such as enzyme catalysis, molecular recognition, crystal engineering, and drug design.[1−4] The H-bond is usually presented in the form of X-H···Y, where X and Y are highly electronegative elements such as O, N, and F. While the H-bond is typically conceived as intermolecular interaction between pairs of molecules, it can occur as intramolecular interaction when two polar functional groups are simultaneously present within the same molecule.

Intramolecular hydrogen bonds are widespread in organic and biological molecules. They stabilize molecular conformations, tune the folding patterns and the way in which they interact with each other or with the solvent, and affect molecular physicochemical properties such as membrane permeability, water solubility, and lipid solubility.[5−9] The formation or disruption of intramolecular H-bonds is often used as a design strategy to modulate chemical and biological properties of interest, such as new materials and drugs.[10−13] On the other hand, the design strategies also require an assessment of intramolecular H-bond strength or its formation probability, which is a subtle balance governed by conformational flexibility, steric strain, and polarity of functional groups. Recently, several theoretical and experimental methods have been proposed to estimate the strength of intramolecular H-bonds.[14−16]

Received: July 11, 2023
Revised: October 7, 2023
Accepted: October 9, 2023
Published: October 24, 2023

Aminoalcohols are important building blocks of biological molecules which play a role in life-related processes such as transmission of nerve impulses or cell membranes. This particular system possesses a flexible backbone with two polar functional groups whose conformation strongly depends on intramolecular H-bond formed between −OH and $-NH_2$ groups. For the straight-chain linear aminoalcohols, $NH_2(CH_2)_nOH$, in which the H-bonded donor and acceptor are separated by a variable linker of the $-CH_2$ group, such as 2-aminoethanol (2-AE), 3-aminopropanol (3-AP), 4-aminobutanol (4-AB) and 5-aminopentanol (5-AP), can be used as a prototype for investigating the effect of conformational flexibility on intramolecular H-bond. Undoubtedly, the properties of the compounds should be mediated by the linking number of methylene fragments.

Intramolecular H-bonds in aminoalcohols $NH_2(CH_2)_nOH$ have been the subject of many experimental and theoretical studies. The levels of theory range from Hartree−Fock, MP2, B3LYP and CCSD(T),[17−21] and spectral techniques include microwave spectroscopy, low-temperature matrix infrared spectroscopy, and gas-phase infrared spectroscopy.[22−31] It was shown that only the conformer with the O−H···N intramolecular hydrogen bond was identified in the gas phase although theoretical calculation predicted that another conformer with the N−H···O intramolecular H-bond should exist. In addition, compared to n = 2, the O−H···N intramolecular H-bond is much stronger in n = 3, indicating that the strength of intramolecular H-bond increases as the backbone chain gets longer. This can easily be understood when considering that increasing the chain length will lead to an increase in the flexibility of the chain linking the NH_2 and OH groups. A more flexible chain will be more favorable for orientating two functional groups to maximize the intramolecular H-bond strength. Recently, using microwave spectroscopy under supersonic jet cooling condition of 2 K rotational temperature, Lavrich et al. conducted a series of investigations on intramolecular H-bonded conformations of linear aminoalcohols n = 2−5, showing that n = 4 yields the strongest intramolecular H-bond.[25,26,29,31] In addition, using high-level G4 ab initio calculations, Lamsabhi et al. investigated the characteristics of intramolecular H-bonds in aminoalcohols of n = 2−7 and suggested that the strength of intramolecular H-bonds goes through a maximum at n = 4 with a seven-membered ring.[19] It is known that conformational distributions under supersonic jet cooling conditions are different from room temperature, and accurate description of the characteristics of weak noncovalent interaction is still a challenge for quantum chemistry calculation. To get a better understanding on the effect of chain length on the strength of intramolecular H-bond and the formation probability for different ring sizes, we systematically investigate gas-phase Raman spectra of a series of linear aminoalcohols $NH_2(CH_2)_nOH$ (n = 2−5) in the N−H and O−H stretching regions at different temperatures from room temperature 25 to 65 °C.

Vibrational spectroscopy, including infrared and Raman spectroscopy, is a powerful tool for identifying molecular conformations and intramolecular H-bond. It is known that vibrational frequencies of functional groups are sensitive to conformational changes, and different vibrational frequencies directly correspond to different conformers, which provide the basis for experimental studies. On the other hand, when an intramolecular H-bond is formed, it can cause a substantial conformational change accompanied by a red shift in vibrational frequency. Compared to the gas phase, liquid- and solid-state vibrational spectroscopies are often disturbed by molecular association and barely considered as a free molecule. Therefore, the gas-phase vibrational spectra are more advantageous in providing intrinsic information on intramolecular interaction due to being free from intermolecular interaction.

Compared to gas-phase infrared spectroscopy, the band shape of gas-phase Raman spectroscopy is more narrow and separated and thus can reduce rovibrational substructure and decrease spectral overlapping in a particularly effective way, more favorable in distinguishing different conformers. This is because infrared and Raman spectroscopies have different transition selection rules. The former consists of three P, Q, and R branches from $\Delta J = 0, \pm 1$ transitions, whereas the latter mainly consists of the Q branch from the $\Delta J = 0$ transition. Recently, based on gas-phase supersonic jet Raman spectroscopy and theoretical calculations, Suhm et al. conducted a benchmarking investigation on the correlations between O−H stretching frequency and subtle H-bond in a series of vicinal diols, and identified their H-bonded and free conformers.[32,33]

Conventional gas-phase spontaneous Raman spectroscopy is generally weak, which limits its application to some extent. It is particularly worth mentioning that the detection of gas-phase Raman spectra has been significantly improved by Hippler et al. and Hu et al. using cavity-enhanced Raman spectroscopy (CERS).[34,35] In this work, we employed photoacoustic Raman spectroscopy (PARS) technique to obtain gas-phase Raman spectra of four aminoalcohols $NH_2(CH_2)_nOH$ (n = 2−5). The PARS is a combination of stimulated Raman scattering and sensitive photoacoustic spectroscopy. It has very high sensitivity and spectral resolution, especially suitable for measuring gas-phase Raman spectra of low-volatility aminoalcohols.

EXPERIMENTAL METHODS

The basic theory and experimental setup of PARS have been fully described in previous studies.[36−39] Here, only a simple description is shown. When the frequency difference between two laser beams (pump and Stokes beams) is resonant with a Raman-active vibrational transition, a stimulated Raman scattering process occurs, and the ground-state molecules are transferred to vibrationally excited states. Then, intermolecular collisions cause vibrational excitation energy to convert to local heating, creating a sound wave that is detected by a microphone. The sensitivity of PARS is greatly increased compared to the conventional spontaneous Raman measurement.

In the experiment, the second-harmonic output of 532.1 nm from a pulsed Nd:YAG laser (line width of 1.0 cm^{-1}, pulse width of 10 ns) was split into two beams by a quartz wedge. About 90% of the 532.1 nm laser energy directly entered into a dye laser system (ND6000, line width 0.05 cm^{-1}) for generating a tunable Stokes beam (625−637 nm), and the remainder was used as a pump beam for PARS. The two linearly polarized laser beams were focused in the center of a photoacoustic cell with a counterpropagating configuration. The photoacoustic signal is averaged by a boxcar integrator to obtain a PARS spectrum. The energies of the pump and Stokes beams are typically 20 and 10 mJ/pulse, respectively. The obtained PARS spectrum is normalized relative to the intensity of the Stokes beam. The wavelengths of both beams are

https://doi.org/10.1021/acs.jpca.3c04674
J. Phys. Chem. A 2023, 127, 9013−9021

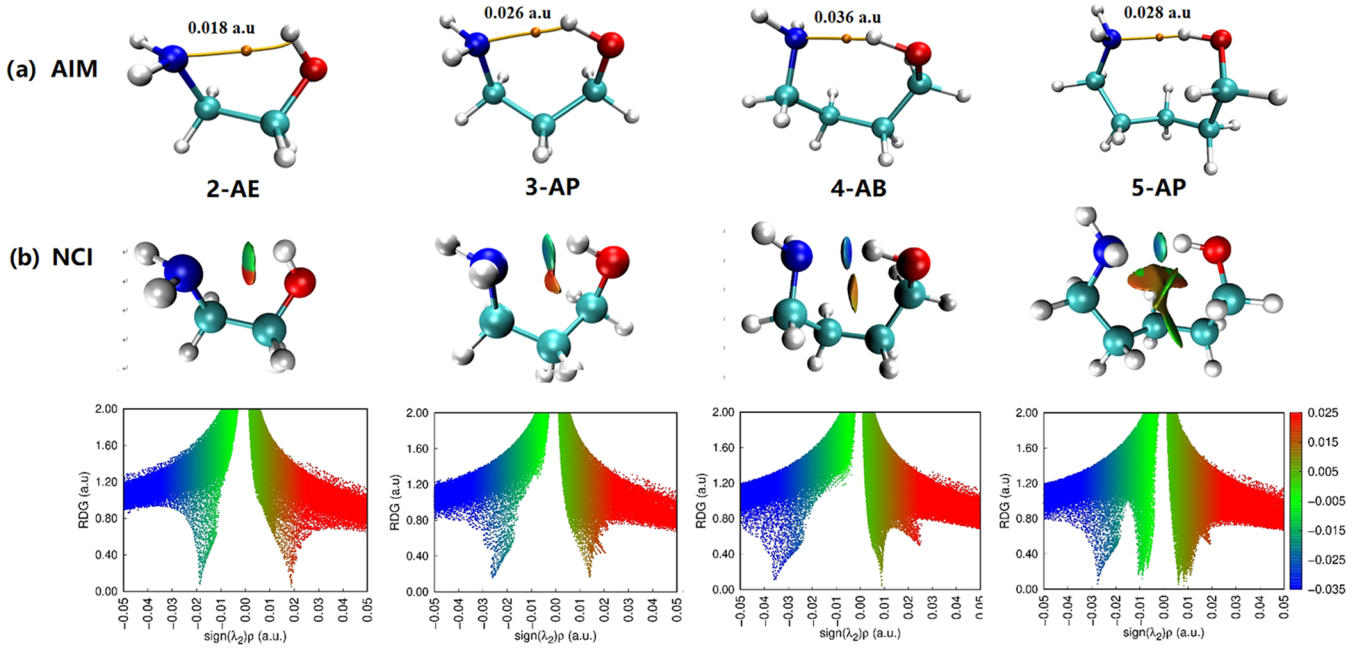

Figure 1. (a) AIM molecular graphs for the most stable conformers of four aminoalcohols $NH_2(CH_2)_nOH$ (n = 2−5) obtained at the M062*X*/6-311++G(d,p) level. The color coding is gray white = H, light blue = C, dark blue = N, red = O, and orange = bond critical point. For visual clarity, only the bond critical point (BCP) between H and N is shown, while the others were deleted. (b) NCI isosurfaces for the most stable intramolecular H-bonded conformers of four aminoalcohols obtained at the M062*X*/6-311++G(d,p) level. The range of sign(λ_2) × ρ(r) used for the plots is −0.035 to +0.025 au at s = 0.4 au. G and g = gauche (∼60°), and T and *t* = trans (∼180°); the prime (′) indicates a negative value of 60°.

calibrated by a wavelength meter with an accuracy of 0.005 nm.

2-Aminoethanol (2-AE), 3-aminopropanol (3-AP), 4-aminobutanol (4-AB), and 5-aminopentanol (5-AP) were obtained from Aladdin Company with spectral grade and were used without further purification. Similar to the method of removing water from ethylene glycol,[40] all of the aminoalcohol samples were dried over a molecular sieve for 24 h and then placed in a glass tube on a vacuum line and degassed by several freeze−pump−thaw cycles. Owing to the low vapor pressure of aminoalcohols, about 0.1 Torr at 20 °C for 2-AE and lower for other aminoalcohols, it was necessary to dry the sample very well to prevent the spectra from being interfered by H_2O. To remove water vapor as much as possible, the cell and sample were evacuated on a vacuum line for about 2 h. To enhance the photoacoustic signal at low pressure, a buffer gas of 20 Torr argon was added to the photoacoustic cell for all of the spectra. When conducting variable temperature PARS experiments, the whole photoacoustic cell was bound with a 500 W heat band. Owing to the limitations of the response of our microphone, the temperature was kept below 70 °C.

■ COMPUTATIONAL DETAILS

All calculations were performed with the Gaussian 16 suite of programs,[41] including geometry optimizations, relative energies, and harmonic vibrational frequencies. The vibrational frequency analyses were used to verify that all optimized structures correspond to the true minima on the potential energy surface and compute the zero point energy (ZPE). The initial conformation searching was performed by a semi-empirical method of PM7 based on Molclus code.[42] Then, those low-energy conformations were selected for subsequent optimizations using the density functional M062X with the 6-311++G(d,p) basis set. The M062X functional was chosen because it performed well in characterizing weak noncovalent interaction in previous studies.[43] Also, the density functional D3-B3LYP/6-311++G(d,p) was performed to compare with M062*X*/6-311++G(d,p). To obtain more accurate energies, single-point energies were calculated at the MP2/aug-cc-pVTZ level with M062*X*/6-311++G(d,p) optimized geometries and ZPE. The thermodynamic data including enthalpy (H), entropy (S), and Gibbs free energy (G) were calculated by Shermo program (version 2.3.5) using thermal correction at the M062*X*/6-311++G(d,p) level and electronic energies at the MP2/aug-cc-pVTZ level.[44]

In addition, intramolecular H-bonding interactions were characterized by atoms in molecules (AIM)[45] and noncovalent interaction (NCI) theories,[46] respectively, which are topological methods based on the electron density. AIM identifies bond critical points (BCPs) as stationary points of the electron density $\rho(r)$, which corresponds to $\nabla\rho(r) = 0$ and can be used as a criterion for the hydrogen bond. Generally, the larger the value of ρ, the stronger the H-bonding interaction. In NCI, noncovalent interactions are identified as areas of low electron density and low reduced density gradient, $s = \frac{1}{2(3\pi^2)^{1/3}} \frac{|\nabla\rho(r)|}{\rho(r)^{4/3}}$. The electron density is multiplied by the sign of the second Hessian eigenvalue, λ_2, to characterize the location, strength, and type of weak interaction. $\lambda_2 < 0$ corresponds to a bonding interaction, whereas $\lambda_2 > 0$ corresponds to a repulsive interaction. Results from NCI calculations can be visualized by mapping the color-coded area according to the values of sign(λ_2) × $\rho(r)$. Blue represents strong attractive interactions and green weaker interactions, whereas red represents repulsive interactions. The color code is only within the program used, and other programs may use other colors. Both

https://doi.org/10.1021/acs.jpca.3c04674
J. Phys. Chem. A 2023, 127, 9013−9021

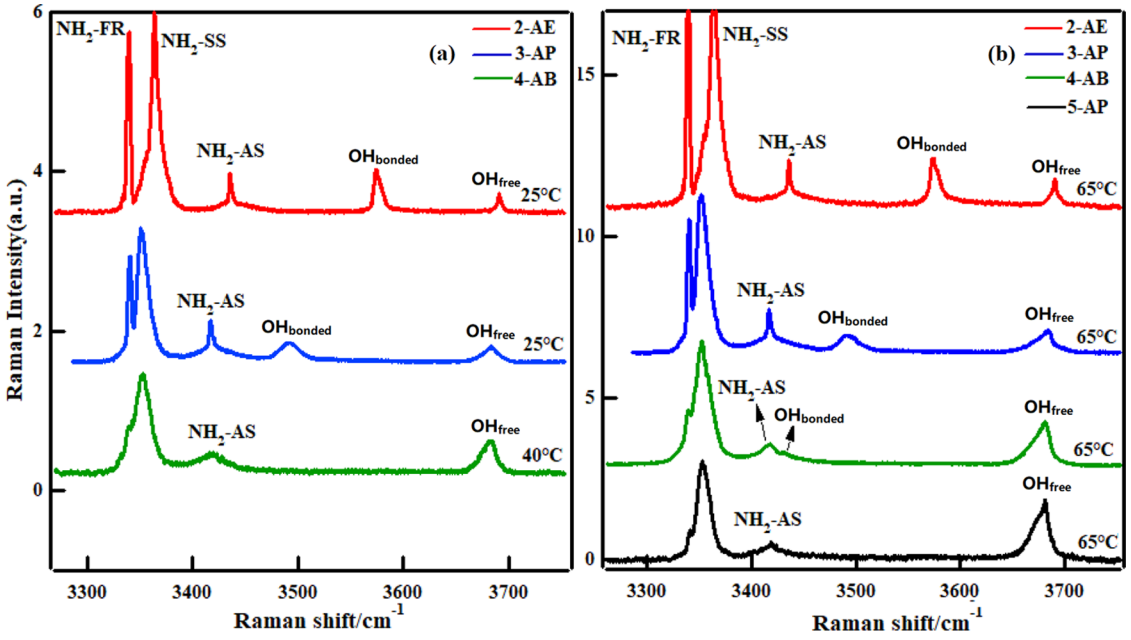

Figure 2. Gas-phase Raman spectra of four aminoalcohols in the N−H and O−H stretching regions at different temperatures. (a) Low temperature and (b) high temperature. The OH_{bonded} denotes the O−H stretching band from the O−H···N intramolecular H-bonded conformer, and the OH_{free} denotes that of the free-OH conformer. NH_2-SS: NH_2 symmetric stretching; NH_2-AS: NH_2 antisymmetric stretching; NH_2-FR: the overtone of the NH_2 bending mode that is enhanced due to Fermi resonance with NH_2-SS.

AIM and NCI were carried out by the Multiwfn program and visualized using VMD software (version 1.9.3).[47]

RESULTS AND DISCUSSION

Conformational Analysis. 2-Aminoethanol (2-AE) is characterized by three independent torsional angles (C−C−N−lp, N−C−C−O, and C−C−O−H; lp = lone pair), giving a total of 3^3 = 27 staggered conformations. Some of the structures are degenerated due to symmetry, and then the number of independent conformations is 14. In the case of 3-aminopropanol(3-AP), 4-aminobutanol(4-AB), and 5-aminopentanol(5-AP), their geometries are characterized by 4, 5, and 6 independent torsional angles, respectively, giving the possible conformations of 3^4, 3^5, and 3^6 that complicate the structural studies.

In this article, the following notations for the conformation description are used. Taking 2-AE as an example, the uppercase letters (G and T) refer to the orientation of the heavy atom backbone (N−C−C−O) and the lowercase letters refer to the orientation adopted by the C−C−N−lp and C−C−O−H axes. G and g = gauche (∼60°) and T and t = trans (∼180°); the prime (′) indicates a negative value of 60° for the corresponding dihedral angles. Similarly, for 3-AP, 4-AB, and 5-AP, the orientations of the heavy atom backbone are indicated by uppercase letters G, G′, and T, while those of C−C−N−lp and C−C−O−H axes are indicated by lowercase letters g, g′, or t.

Figure 1 shows the most stable conformer of four aminoalcohols $NH_2(CH_2)_nOH$ (n = 2−5) along with their AIM and NCI analyses, and the optimized geometries of other low-energy conformers are presented in the Supporting Information (Figure S1). From Figure 1, it can be seen that for each aminoalcohol n = 2−5, the most stable conformers are stabilized by an O−H···N intramolecular H-bond, corresponding to five-membered, six-membered, seven-membered, and eight-membered rings, respectively. On the other hand, both AIM and NCI analyses show that the strength of the intramolecular H-bond significantly depends on the carbon chain length. It can be seen from AIM analysis that the electron density in the bond critical point (BCP) is 0.018, 0.026, 0.038, and 0.028 au in 2-AE, 3-AP, 4-AB, and 5-AP, respectively, indicating that from n = 2−4, the strength of intramolecular hydrogen bond goes up as the chain length increases; whereas from n = 4−5, it decreases as the chain further gets longer. Therefore, according to the calculations, n = 4 corresponds to the strongest intramolecular H-bond. The NCI calculations give similar results. Table S1 lists the calculated geometrical parameters for the O−H···N intramolecular H-bond of four aminoalcohols n = 2−5 at different theoretical levels including M062X, B3LYP-D3, and MP2. It can be seen that both the calculated shortest H···N distance and the largest angle θ (∠OHN) are at n = 4. Therefore, these results are consistent with previous theoretical calculations for n = 2−7 that the strongest intramolecular H-bond occurs in n = 4.[19]

To assist the assignment of experimental spectra, the calculated N−H and O−H stretching vibrational frequencies for low-energy conformers of n = 2−5 are presented in Table S2 (Supporting Information), in which the relative energies and Boltzmann distributions as well as Gibbs free energies for each conformer are also listed. The general trend for the stability of conformers is in good agreement with the previous calculated results.[20−22] The Boltzmann distributions (%) were obtained by performing a statistical thermodynamic population analysis at 298 K. The calculated Boltzmann populations for the most stable conformers are 67.5, 76.1, 71.2, and 10.6% for 2-AE, 3-AP, 4-AB, and 5-AP, respectively. The sharp decrease in conformational population of 5-AP is due to a decrease in intramolecular H-bond strength and, moreover, due to a sharp increase in the number of possible conformations.

Gas-Phase Raman Spectra of Aminoalcohols. Figure 2 presents the gas-phase Raman spectra of four aminoalcohols

https://doi.org/10.1021/acs.jpca.3c04674
J. Phys. Chem. A 2023, 127, 9013−9021

$NH_2(CH_2)_nOH$ (n = 2−5) in the N−H and O−H stretching regions at different temperatures. Table 1 summarizes the observed band positions along with the calculated frequencies and Raman activities. Combined with the calculated results, we assign the observed spectra.

Table 1. Observed and Calculated Vibrational Frequencies (cm^{-1}) of Four Aminoalcohols in the N−H and O−H Stretching Regions

compounds	υ_{obs} [a]	υ_{cal} [b]	Raman activity [c]	assignments [d]
2-AE	3335	3314		NH_2-FR
	3364	3334	114.34	NH_2-SS
	3435	3417	58.23	NH_2-AS
	3574	3585	41.48	OH_{bonded}-g′Gg′
	3690	3686	94.09	OH_{free}-gGt/tGt
3-AP	3340	3310		NH_2-FR
	3351	3317	121.50	NH_2-SS
	3417	3398	67.06	NH_2-AS
	3492	3524	58.64	OH_{bonded}-gG′Gg′
	3683	3684	99.86	OH_{free}-gG′G′t
4-AB	3339	3301		NH_2-FR
	3353	3316	132.93	NH_2-SS
	3417	3393	53.58	NH_2-AS
	3431	3382	88.78	OH_{bonded}-g′GG′Gg′
	3681	3680	120.52	OH_{free}-gG′TGt
5-AP				
	3341	3301		NH_2-FR
	3351	3311	109.52	NH_2-SS
	3418	3389	67.35	NH_2-AS
	unobserved	3457	90.53	OH_{bonded}-gG′TG′Gg
	3681	3681	117.25	OH_{free}-g′G′TTG′t

[a]For 2-AE and 3-AP, all of the bands were identified at both 25 and 65 °C. For 4-AB, all of bands were identified at 40 and 65 °C except the 3431 cm^{-1} band at only 65 °C. For 5-AP, all of the bands were identified at 65 °C. [b]Harmonic frequencies calculated at the M062X/6-311++G(d,p) level and the frequency scale factor of 0.939 were used to assist the observed N−H and O−H stretching vibrations. The calculated NH_2 bending mode was multiplied by 2 to obtain the calculated positions with no scale. [c]Raman activity was calculated at the M062X/6-311++G(d,p) level. [d]NH_2-SS: NH_2 symmetric stretching; NH_2-AS: NH_2 antisymmetric stretching; NH_2-FR: the overtone of the NH_2 bending mode that is enhanced due to Fermi resonance with NH_2-SS.

As shown in Figure 2(a), the gas-phase Raman spectra of 2-AE at room temperature 25 °C shows three intense bands at 3335, 3364, and 3435 cm^{-1}, respectively. According to calculations, these three bands can be assigned to NH_2 bending overtone, symmetric stretching (SS), and antisymmetric stretching (AS), respectively. The NH_2 bending overtone was calculated at 3314 cm^{-1}(2*1657), which is enhanced by Fermi resonance with NH_2 symmetric stretching due to their close frequency and the same symmetry, and called as NH_2-FR here. Such Fermi-resonance pairs were recently identified in size-specific infrared spectra of ammonia clusters combined with quantum chemistry calculations.[48] The above three N−H bands are present in gas-phase Raman spectra of all four aminoalcohols n = 2−4 at different temperatures with similar band positions and relative intensities. Since theoretical calculations show that the N−H stretching vibrations are not sensitive to conformational changes of aminoalcohols (Table S2), we mainly focus on the O−H stretching spectra in the following text.

For both 2-AE and 3-AP, two O−H stretching bands can be clearly observed in the gas-phase Raman spectra, as can be seen from Figure 2(a). According to theoretical calculations, the higher frequencies at 3690 and 3683 cm^{-1} can be assigned to the stretching vibrations from free-OH conformers in n = 2 and 3, respectively, and labeled as OH_{free}. The lower frequencies were located at 3574 and 3492 cm^{-1}. It is known that the red shifts of the O−H stretching frequency are spectroscopic signatures of H-bond formation. So the bands at 3574 and 3492 cm^{-1} can be assigned to the most stable conformers with the O−H···N intramolecular H-bond and labeled as OH_{bonded}. It can be seen that the red shifts ($\Delta\upsilon$=OH_{bonded} - OH_{free}) are 116 $cm^{-1}$and 191 cm^{-1} in n = 2 and 3, respectively, in good agreement with previous measurements from gas-phase infrared spectra.[22,24,27]

In the case of 4-AB and 5-AP, the gas-phase Raman spectra at room temperature are too weak to be detected due to their lower volatility. To enhance the signal, the spectrum of 4-AB was measured at 40 °C, whereas for 5-AP, it is still difficult to obtain a spectrum at this temperature. Since 40 °C is only 15 °C higher than room temperature, it should not have a fundamental effect on the spectral intensity or conformational populations. As can be seen from Figure 2(a), the n = 4 spectrum shows only one high-frequency O−H stretching band located at ∼3681 cm^{-1}, which corresponds to the free-OH conformers, whereas the remaining three bands at 3339, 3353, and 3417 cm^{-1} come from N−H bands. Therefore, the OH_{bonded} band was not obviously observed due to the low signal level. This also indicates that the population or the probability from the OH_{bonded} conformer significantly decreases near room temperature compared to n = 2 and 3.

Table 1 lists the calculated Raman activities of OH_{bonded} and OH_{free} vibrations. It can be seen that the Raman activity of OH_{bonded} is weaker than that of OH_{free} with the OH_{bonded}/OH_{free} ratios of 0.44, 0.58, 0.73, and 0.76 for n = 2−5, respectively. Therefore, the calculated weaker Raman activities

Table 2. Calculated Entropy ΔS (cal/mol/K), Enthalpy ΔH (kcal/mol), and Gibbs Free Energy ΔG (kcal/mol) between Intramolecular H-Bonded Conformer and Open-Chain Conformer at Different Temperatures

	0 K [a]			298 K [a]			338 K [a]		
compound	ΔS	ΔH	ΔG	ΔS	ΔH	ΔG	ΔS	ΔH	ΔG
2-AE	0	−2.69	−2.69	−2.03	−2.99	−2.38	−2.14	−3.02	−2.30
3-AP	0	−3.34	−3.34	−4.27	−3.87	−2.60	−4.45	−3.92	−2.42
4-AB	0	−3.41	−3.41	−5.19	−4.03	−2.49	−5.40	−4.10	−2.28
5-AP	0	−3.38	−3.38	−6.77	−3.95	−1.94	−6.80	−3.96	−1.66

[a]Calculated from MP2/aug-cc-pVTZ electronic energies with ZPVE, enthalpy, and entropy contributions calculated using M062X/6-311++G(d,p).

https://doi.org/10.1021/acs.jpca.3c04674
J. Phys. Chem. A 2023, 127, 9013−9021

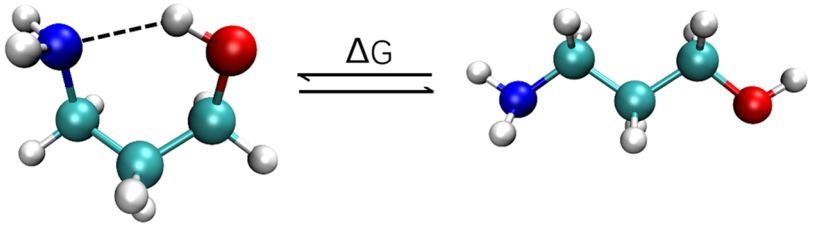

Figure 3. Illustration of the conformational equilibrium between intramolecular H-bonding and open-chain forms with 3-AP as an example.

decrease the observations of OH_{bonded} vibration in experiment, but it does not change the trend that the population of the OH-bonded conformer significantly decreases in n = 4 compared to n = 2 and n = 3, as shown in Figure 2(a), indicating that intramolecular H-bond formation significantly decreases as the backbone chain gets longer.

According to the calculated band positions listed in Table 2, the red-shifted OH_{bonded} and NH_2 antisymmetric stretching vibrations are very close in n = 4, and so they may overlap. To demonstrate this possibility, the gas-phase Raman spectrum of n = 4 was measured at 65 °C to obtain higher signal-of-noise and the spectra of n = 2, 3, 5 were also measured at this temperature, as shown in Figure 2(b). It can be seen that a very weak shoulder at ∼3431 cm^{-1} is observed in n = 4 compared to the spectra at 40 °C, which is overlapped with broad NH_2-AS band centered at ∼3417 cm^{-1}. The shoulder at ∼3431 cm^{-1} can be assigned to the OH_{bonded} although the calculated OH_{bonded} band is at 3382 cm^{-1} (the difference is 49 cm^{-1}). For n = 2 and 3, the observed and calculated OH_{bonded} bands also differ by 11 and 32 cm^{-1}, respectively, as shown in Table 1. Compared to free OH, the observed red shift is 249 cm^{-1} in n = 4.

For n = 5, only one high-frequency OH_{free} band was observed at ∼3681 cm^{-1}, indicating that the probability for intramolecular H-bond further decreases in n = 5 compared to n = 4. It should be mentioned that due to high conformational flexibility of linear aminoalcohols n = 2−5, the observed OH_{free} bands at room temperature may be contributed by more than one conformers with close OH stretching frequency, especially for n = 5, as shown in Table S2. In a recent microwave study, two conformers were identified for 5-AP in supersonic cooling conditions due to higher conformational flexibility, whereas for n = 2−4, only one conformer was identified.[29]

Unlike the intermolecular H-bond, the temperature does not significantly change the intramolecular H-bond strength, especially in a limited temperature range such as that in our experimental condition. As can be seen from Figure 2, the red shifts of OH_{bonded} bands of n = 2 and n = 3 are similar at 25 and 65 °C. In addition, the red shift of 249 cm^{-1} in n = 4 at 65 °C is much larger than those of 116 and 191 cm^{-1} in n = 2 and n = 3, respectively. Therefore, the intramolecular H-bond in n = 4 is much stronger than that in n = 2 and n = 3, in good agreement with AIM and NCI analyses and microwave investigation under supersonic jet cooling conditions that the strongest intramolecular H-bond exists in n = 4.[26] The largest red shift means the strongest H-bond, but it does not mean the most favorable formation probability in n = 4 since the latter is dependent on the temperature at which the molecules are. As seen from the OH_{bonded} intensity of n = 2−4 in Figure 2(a), it can be seen that the intramolecular H-bond probability for n = 2 and n = 3 is much larger than that for n = 4, whereas from a view of intramolecular H-bond strength, n = 4 and n = 3 are much stronger than n = 2. According to the calculations (Table S1), the O−H···N intramolecular H-bonding angle is about 115°, which is far from an optimal 180° and thus the H-bond is expected to be weak in such a five-membered ring. Considering the factors of both strength and probability, n = 3 should be the favorable chain length to form an intramolecular H-bond in linear aminoalcohols n = 2−5 near room temperature, indicating that a sort of balance between higher flexibility of a hydrocarbon skeleton and steric hindrance of functional groups is reached in n = 3. Such result is in good agreement with statistical analysis of crystal structures in the Cambridge Structural Database (CSD) that the probability of intramolecular H-bond formation is far greater for a six-membered ring than for any other systems such as five-membered, seven-membered, and eight-membered rings.[52]

In addition, comparing the Raman spectra of n = 2 and n = 3 at 25 and 65 °C in Figure 2, it can be seen that with the increasing temperature, the OH_{bonded} band decreases and the OH_{free} band increases. From 25 and 65 °C, the intensity ratio of OH_{bonded}/ OH_{free} changes from 2.18 to 1.78 for n = 2 (1.78/2.18 = 0.81) and from 1.29 to 0.81 for n = 3 (0.81/1.29 = 0.63), where the intensity was measured as maximum height of the peak. The greater the change in intensity ratios of OH_{bonded}/ OH_{free}, the greater the energy difference between the two conformers and then the stronger the intramolecular hydrogen bond. Therefore, the intramolecular H-bond in n = 3 is stronger than that in n = 2. Since we only measured the gas-phase Raman spectra of n = 2 and n = 3 at two temperatures, the data on intramolecular H-bond strength were not obtained. Recently, Siewert et al. conducted a detailed thermodynamic evaluation of the H-bond strength in a series of 1,2-aminoalcohols and 2,1-aminoalcohols and the O−H···N intramolecular bond strength was assessed to be at the level of $\Delta H = -11 \pm 3$ kJ/mol.[16]

Calculated Thermodynamic Data. Understanding why the increase of conformational flexibility limits the formation of intramolecular H-bonds will aid in rational design of medicine and ligands for protein. According to Ruzicka's intuition,[49] the probability of the chain terminals coming close enough to each other for the reaction to occur should decrease on increase of the chain length connecting the reacting groups. In terms of entropy, this implies that a negative entropy contribution occurs when the open chain is converted into a closed ring.[50,51] Similar understanding can be applied to intramolecular H-bond formation; the structure in which the torsional motions of the backbone chain become restricted is entropically unfavorable when the intramolecular H-bond is formed. The more freely the bond rotates, the greater its torsional entropy.

To reveal the origin of optimal chain length for intramolecular H-bond in linear aminoalcohols $NH_2(CH_2)_nOH$ (n = 2−5), the thermodynamic parameters between intramolecular H-bonded and open-chain conformers were

https://doi.org/10.1021/acs.jpca.3c04674
J. Phys. Chem. A 2023, 127, 9013−9021

calculated, including entropy, enthalpy, and Gibbs free energy. The open-chain conformer was chosen as a reference, in which the backbone carbon chain was expanded without intramolecular H-bond and then the hydroxyl and amino groups are the most distant from each other, as shown in Figure 3. Such open-chain reference systems were often used to estimate the strength of the intramolecular H-bond in previous studies.[15,16] Table S3 summarizes the calculated thermodynamic parameters between intramolecular H-bonded and open-chain conformers at 0−400 K with an interval of 100 K, whereas those at specific temperatures of 0, 298, and 338 K are listed in Table 2, including the changes in entropy (ΔS) and enthalpy (ΔH) as well as Gibbs free energy (ΔG). As can be seen from Table S3, the minimum Gibbs free energy (ΔG) is dependent on the temperature. It occurs in n = 4 under low temperature T < 200 K, whereas it occurs in n = 3 at 200 K ≤ T < 400 K, and occurs in n = 2 at T ≥ 400 K. For this reason, n = 4 was observed as a single conformer with the strongest intramolecular H-bond under supersonic jet cooling conditions.[26] Since our experimental temperature ranges from room temperature 298 to 338 K, the Gibbs free energy optimum occurs in n = 3 according to the calculations in Table 2.

As shown in Table 2, using thermal correction at the M062X/6-311++G(d,p) level and electronic energies at the MP2/aug-cc-pVTZ level, the calculated enthalpy change (ΔH) at 298 K is −2.98 kcal/mol (equals −12.5 kJ/mol) for 2-AE, which is very close to the value of −11.7 kJ/mol calculated at high-level G4 method.[16] The calculated entropy change (ΔS) at 298 K is −2.03 cal/mol/K for n = 2, whereas for n = 3, 4, and 5, the values are −4.27, −5.18, and −6.77 cal/mol/K, indicating that an unfavorable entropy contribution increases with the backbone chain length. On the other hand, the calculated enthalpy changes (ΔH) are −2.98, −3.86, −4.03, and −3.95 kcal/mol in n = 2−5, respectively. This results in a minimum of total Gibbs free energy ($\Delta G = \Delta H$-TΔS) for n = 3 with a value of −2.60 kcal/mol. It is known that the reactions in nature always proceed in the direction of a decrease in free energy. Therefore, from a view of chemical reaction, above-calculated thermodynamic data indicate that the most favorable chain length for intramolecular H-bond formation occurs in n = 3, which corresponds to a six-membered ring in 3-AP, in good agreement with the observed gas-phase Raman spectra in Figure 2 when considering that the intramolecular H-bond strength in n = 4 and n = 3 is stronger than that in n = 2 while the formation probabilities in n = 2 and n = 3 are larger than that in n = 4. As mentioned early, Kuhn et al. investigated many molecular systems containing intramolecular H-bonds from five- to eight-membered rings by searching from Cambridge Structural Database (CSD) and found that a pseudo six-membered ring represents the vast majority of the samples, reflecting that such ring size is the most favorable to form in nature and able to survive in large molecular ensembles.[12,52]

CONCLUSIONS

In this study, we have measured high-resolution gas-phase Raman spectra of four aminoalcohols $NH_2(CH_2)_nOH$ (n = 2−5) in the N−H and O−H stretching regions at different temperatures from room temperature 25 to 65 °C. From the evolution of the observed O−H stretching spectra of the intramolecular H-bonded conformer and free-OH conformer, we have gained insight into the dependence of intramolecular H-bond on chain length at molecular level. Combined with quantum chemistry calculations, it is shown that the strongest intramolecular H-bond exists in n = 4, but the entropy drives the Gibbs free energy to be optimal for the intramolecular H-bonded conformation with n = 3 at room temperature. This implies that the six-membered ring intramolecular H-bond is the most favorable to form in linear aminoalcohols at room temperature. These results will provide a useful basis for its more directed and rational use of intramolecular H-bond in medicinal chemistry, drug design, and new materials.

ASSOCIATED CONTENT

Supporting Information

The Supporting Information is available free of charge at https://pubs.acs.org/doi/10.1021/acs.jpca.3c04674.

Figure S1. Optimized geometry for low-energy conformers of four aminoalcohols $NH_2(CH_2)_nOH$ (n = 2−5) along with their NCI analysis; Table S1. Calculated geometrical parameters for O−H···N intramolecular hydrogen bond of the most stable conformers of four aminoalcohols. Table S2. Calculated O−H and N−H stretching vibrational frequencies, relative energies (kcal/mol), Gibbs free energy, and Boltzmann populations (%) of low-energy conformers for four aminoalcohols. Table S3. Calculated entropy ΔS, enthalpy ΔH, and Gibbs free energy ΔG between intramolecular H-bonded conformer and open-chain conformer at different temperatures (PDF)

AUTHOR INFORMATION

Corresponding Authors

Yuanqin Yu − *School of Physics and Optoelectronic Engineering, Anhui University, Hefei 230601, China;* orcid.org/0000-0001-7647-8404; Email: yyq@ahu.edu.cn

Shilin Liu − *Hefei National Laboratory for Physical Sciences at the Microscale, iChEM (Collaborative Innovation Center of Chemistry for Energy Materials), Department of Chemical Physics, University of Science and Technology of China, Hefei 230026, China*; Email: slliu@ustc.edu.cn

Authors

Yuhui Li − *School of Physics and Optoelectronic Engineering, Anhui University, Hefei 230601, China*

Xinlang Yang − *Hefei National Laboratory for Physical Sciences at the Microscale, iChEM (Collaborative Innovation Center of Chemistry for Energy Materials), Department of Chemical Physics, University of Science and Technology of China, Hefei 230026, China*

Xiaoguo Zhou − *Hefei National Laboratory for Physical Sciences at the Microscale, iChEM (Collaborative Innovation Center of Chemistry for Energy Materials), Department of Chemical Physics, University of Science and Technology of China, Hefei 230026, China;* orcid.org/0000-0002-0264-0146

Rui Zhang − *School of Physics and Optoelectronic Engineering, Anhui University, Hefei 230601, China;* orcid.org/0000-0002-5206-5434

Jin Sun − *School of Physics and Optoelectronic Engineering, Anhui University, Hefei 230601, China*

Complete contact information is available at: https://pubs.acs.org/10.1021/acs.jpca.3c04674

Notes

The authors declare no competing financial interest.

■ ACKNOWLEDGMENTS

This work was supported by the National Natural Science Foundation of China (NSFC, 21873002, 22073088, 12374001, 2202780, and11874067).

■ REFERENCES

(1) Jeffrey, G. A.; Saenger, W. *Hydrogen Bonding in Biological Structures*; Springer Science & Business Media, 1990.
(2) Li, G.; Zhang, Y.-Y.; Li, Q.; Wang, C.; Yu, Y.; Zhang, B.; Hu, H.-S.; Zhang, W.; Dai, D.; Wu, G.; et al. Infrared spectroscopic study of hydrogen bonding topologies in the smallest ice cube. *Nat. Commun.* **2020**, *11* (1), 5449.
(3) Jiang, S.; Su, M.; Yang, S.; Wang, C.; Huang, Q.-R.; Li, G.; Xie, H.; Yang, J.; Wu, G.; Zhang, W.; et al. Vibrational Signature of Dynamic Coupling of a Strong Hydrogen Bond. *J. Phys. Chem. Lett.* **2021**, *12* (9), 2259−2265.
(4) Desiraju, G. R. *The Weak Hydrogen Bond: In Structural Chemistry and Biology*; Oxford University Press: Oxford, NY, 1999.
(5) Castellano, R. K. Special Issue: Intramolecular Hydrogen Bonding. *Molecules* **2014**, *19* (10), 15783−15785.
(6) Sanchez, G. Introduction to ″Intramolecular Hydrogen Bonding 2018″. *Molecules* **2019**, *24* (16), 2858.
(7) Coimbra, J. T. S.; Feghali, R.; Ribeiro, R. P.; Ramos, M. J.; Fernandes, P. A. The importance of intramolecular hydrogen bonds on the translocation of the small drug piracetam through a lipid bilayer. *Rsc Adv.* **2021**, *11* (2), 899−908.
(8) Tian, S. X.; Yang, J. L. Effects of intramolecular hydrogen bonding on the ionization energies of proline. *Angew. Chem., Int. Ed.* **2006**, *45* (13), 2069−2072.
(9) Guerrero-Corella, A.; Fraile, A.; Aleman, J. Intramolecular Hydrogen-Bond Activation: Strategies, Benefits, and Influence in Catalysis. *ACS Org. Inorg. Au* **2022**, *2* (7), 197−204.
(10) Caron, G.; Kihlberg, J.; Ermondi, G. Intramolecular hydrogen bonding: An opportunity for improved design in medicinal chemistry. *Med. Res. Rev.* **2019**, *39* (5), 1707−1729.
(11) Li, Y.; Sui, J.; Cui, L.-S.; Jiang, H.-L. Hydrogen Bonding Regulated Flexibility and Disorder in Hydrazone- Linked Covalent Organic Frameworks. *J. Am. Chem. Soc.* **2023**, *145* (2), 1359−1366.
(12) Giordanetto, F.; Tyrchan, C.; Ulander, J. Intramolecular Hydrogen Bond Expectations in Medicinal Chemistry. *ACS Med. Chem. Lett.* **2017**, *8* (2), 139−142.
(13) Caron, G.; Ermondi, G. Why we need to implement intramolecular hydrogen-bonding considerations in drug discovery. *Future Med. Chem.* **2017**, *9* (1), 1−5.
(14) Harville, T.; Gordon, M. S. Intramolecular hydrogen bonding analysis. *J. Chem. Phys.* **2022**, *156*, No. 174302.
(15) Jablonski, M. A Critical Overview of Current Theoretical Methods of Estimating the Energy of Intramolecular Interactions. *Molecules* **2020**, *25* (23), 5512.
(16) Siewert, R.; Ludwig, R.; Verevkin, S. P. Non-covalent interactions in molecular systems: thermodynamic evaluation of the hydrogen bond strength in aminoalcohols. *Phys. Chem. Chem. Phys.* **2021**, *23* (44), 25226−25238.
(17) Silva, C. F. P.; Duarte, M.; Fausto, R. A concerted SCF-MO ab initio and vibrational spectroscopic study of the conformational isomerism in 2-aminoethanol. *J. Mol. Struct.* **1999**, *482*, 591−599.
(18) Novakovskaya, Y. V.; Rodnikova, M. N. Ethanolamine: conformational diversity. *Struct. Chem.* **2015**, *26* (1), 177−187.
(19) Lamsabhi, A. M.; Mo, O.; Yanez, M. Perturbating Intramolecular Hydrogen Bonds through Substituent Effects or Non-Covalent Interactions. *Molecules* **2021**, *26* (12), 3556.
(20) Kelterer, A. M.; Ramek, M. Intramolecular hydrogen bonding in 2-aminoethanol, 3-aminopropanol and 4-aminobutanol. *J. Mol. Struc-Theochem* **1991**, *232*, 189−201.
(21) Chang, Y. P.; Su, T. M.; Li, T. W.; Chao, I. Intramolecular hydrogen bonding, gauche interactions, and thermodynamic functions of 1,2-ethanediamine, 1,2-ethanediol, and 2-aminoethanol: A global conformational analysis. *J. Phys. Chem. A* **1997**, *101* (34), 6107−6117.
(22) Thomsen, D. L.; Axson, J. L.; Schroder, S. D.; Lane, J. R.; Vaida, V.; Kjaergaard, H. G. Intramolecular Interactions in 2-Aminoethanol and 3-Aminopropanol. *J. Phys. Chem. A* **2013**, *117* (40), 10260−10273.
(23) Asselin, P.; Madebene, B.; Soulard, P.; Georges, R.; Goubet, M.; Huet, T. R.; Pirali, O.; Zehnacker-Rentien, A. Competition between inter- and intra-molecular hydrogen bonding: An infrared spectroscopic study of jet-cooled amino-ethanol and its dimer. *J. Chem. Phys.* **2016**, *145* (22), No. 224313.
(24) Lane, J. R.; Schroder, S. D.; Saunders, G. C.; Kjaergaard, H. G. Intramolecular Hydrogen Bonding in Substituted Aminoalcohols. *J. Phys. Chem. A* **2016**, *120* (32), 6371−6378.
(25) Khalil, A. S.; Kelterer, A.-M.; Lavrich, R. J. Interplay of Intermolecular and Intramolecular Hydrogen Bonds on Complex Formation: The 3-Aminopropanol-Water van der Waals Complex. *J. Phys. Chem. A* **2017**, *121* (35), 6646−6651.
(26) Hohl, J. A.; Harris, M. W.; Strasser, N.; Kelterer, A.-M.; Lavrich, R. J. Competing Intramolecular Hydrogen Bond Strengths and Intermolecular Interactions in the 4-Aminobutanol-Water Complex. *J. Phys. Chem. A* **2018**, *122* (43), 8505−8510.
(27) Batista, P. R.; Karas, L. J.; Viesser, R. V.; de Oliveira, C. C.; Goncalves, M. B.; Tormena, C. F.; Rittner, R.; Ducati, L. C.; de Oliveira, P. R. Dealing with Hydrogen Bonding on the Conformational Preference of 1,3-Aminopropanols: Experimental and Molecular Dynamics Approaches. *J. Phys. Chem. A* **2019**, *123* (40), 8583−8594.
(28) Cacela, C.; Duarte, M. L.; Fausto, R. Structural and vibrational characterisation of 3-amino-1-propanol a concerted SCF-MO ab initio, Raman and infrared (matrix isolation and liquid phase) spectroscopy study. *Spectrochim Acta A* **2000**, *56* (6), 1051−1064.
(29) Gilbreth, E.; Spann, S.; Lavrich, R. J. Conformational flexibility and hydrogen bonding in 5-aminopentanol. *J. Mol. Spectrosc.* **2022**, *388*, No. 111669.
(30) Liu, Y. Q.; Rice, C. A.; Suhm, M. A. Torsional isomers in methylated aminoethanols - A jet-FT-IR study. *Can. J. Chem.* **2004**, *82* (6), 1006−1012.
(31) Khalil, A. S.; Duguay, T. M.; Lavrich, R. J. Conformation and hydrogen bonding in 4-Aminobutanol. *J. Mol. Struct.* **2017**, *1138*, 12−16.
(32) Hartwig, B.; Suhm, M. A. Subtle hydrogen bonds: benchmarking with OH stretching fundamentals of vicinal diols in the gas phase. *Phys. Chem. Chem. Phys.* **2021**, *23* (38), 21623−21640.
(33) Medel, R.; Suhm, M. A. Predicting OH stretching fundamental wavenumbers of alcohols for conformational assignment: different correction patterns for density functional and wave-function-based methods. *Phys. Chem. Chem. Phys.* **2021**, *23* (9), 5629−5643.
(34) Yang, Q.-y.; Tan, Y.; Qu, Z.-h.; Sun, Y.; Liu, A.-w.; Hu, S.-m. Multiple Gas Detection by Cavity-Enhanced Raman Spectroscopy with Sub-ppm Sensitivity. *Anal. Chem.* **2023**, *95* (13), 5652−5660.
(35) Salter, R.; Chu, J.; Hippler, M. Cavity-enhanced Raman spectroscopy with optical feedback cw diode lasers for gas phase analysis and spectroscopy. *Analyst* **2012**, *137* (20), 4669−4676.
(36) Yu, Y. Q.; Wang, Y. X.; Lin, K.; Hu, N. Y.; Zhou, X. G.; Liu, S. L. Complete Raman Spectral Assignment of Methanol in the C-H Stretching Region. *J. Phys. Chem. A* **2013**, *117* (21), 4377−4384.
(37) Yu, Y. Q.; Wang, Y. X.; Hu, N. Y.; Lin, K.; Zhou, X. G.; Liu, S. L. Cβ-H stretching vibration as a new probe for conformation of n-propanol in gaseous and liquid states. *Phys. Chem. Chem. Phys.* **2016**, *18* (15), 10563−10572.
(38) Yu, Y. Q.; Wang, Y. X.; Lin, K.; Zhou, X. G.; Liu, S. L.; Sun, J. New spectral assignment of n-propanol in the C-H stretching region. *J. Raman Spectrosc.* **2016**, *47* (11), 1385−1393.
(39) Li, Y.; Li, T.; Yu, Y.; Sun, J.; Zhou, X.; Zhang, R.; Liu, S. Vibrational mode-specific polarization effect in circularly polarized

stimulated Raman scattering. *J. Chem. Phys.* **2022**, *157* (20), No. 204201.
(40) Howard, D. L.; Jorgensen, P.; Kjaergaard, H. G. Weak intramolecular interactions in ethylene glycol identified by vapor phase OH-stretching overtone spectroscopy. *J. Am. Chem. Soc.* **2005**, *127* (48), 17096−17103.
(41) Kobayashi, R.; Normand, J.; Raghavachari, K.; Rendell, A. P.; Burant, J. C.; Iyengar, S. S.; Tomasi, J.; Cossi, M.; Millam, J. M.; Klene, M.. et al. Gaussian 16 Rev. C.01; Wallingford, CT, 2016.
(42) Lu, T., http://www.keinsci.com/research/molclus.html, 2016.
(43) Zhao, Y.; Truhlar, D. G. The M06 suite of density functionals for main group thermochemistry, thermochemical kinetics, noncovalent interactions, excited states, and transition elements: two new functionals and systematic testing of four M06-class functionals and 12 other functionals. *Theor. Chem. Acc.* **2008**, *120* (1−3), 215−241.
(44) Lu, T.; Chen, Q. Shermo: A general code for calculating molecular thermochemistry properties. *Comput. Theor. Chem.* **2021**, *1200*, No. 113249.
(45) Bader, R. F. W. *Atoms in Molecules—A Quantum Theory*; Clarendon Press: Oxford, U.K., 1990.
(46) Chaudret, R.; de Courcy, B.; Contreras-Garcia, J.; Gloaguen, E.; Zehnacker-Rentien, A.; Mons, M.; Piquemal, J. P. Unraveling noncovalent interactions within flexible biomolecules: from electron density topology to gas phase spectroscopy. *Phys. Chem. Chem. Phys.* **2014**, *16* (21), 9876−9891.
(47) Lu, T.; Chen, F. Multiwfn: A Multifunctional Wavefunction Analyzer. *J. Comput. Chem.* **2012**, *33*, 580−592.
(48) Zhang, B.; Yang, S.; Huang, Q.-R.; Jiang, S.; Chen, R.; Yang, X.; Zhang, D. H.; Zhang, Z.; Kuo, J.-L.; Jiang, L. Deconstructing Vibrational Motions on the Potential Energy Surfaces of Hydrogen-Bonded Complexes. *CCS Chem.* **2021**, *3* (1), 829−835.
(49) Illuminati, G.; Mandolini, L. Ring-Closure Reactions of Bifunctional Chain Molecules. *Acc. Chem. Res.* **1981**, *14* (4), 95−102.
(50) Galli, C.; Mandolini, L. The role of ring strain on the ease of ring closure of bifunctional chain molecules. *Eur. J. Org. Chem.* **2000**, *2000* (18), 3117−3125.
(51) Colizzi, F.; Hospital, A.; Zivanovic, S.; Orozco, M. Predicting the Limit of Intramolecular Hydrogen Bonding with Classical Molecular Dynamics. *Angew. Chem., Int. Ed.* **2019**, *58* (12), 3759−3763.
(52) Kuhn, B.; Mohr, P.; Stahl, M. Intramolecular Hydrogen Bonding in Medicinal Chemistry. *J. Med. Chem.* **2010**, *53* (6), 2601−2611.

https://doi.org/10.1021/acs.jpca.3c04674
J. Phys. Chem. A 2023, 127, 9013−9021